JOURNAL OF CATALYSIS 89, 478–488 (1984)

Physicochemical Characterization of MoO_3-NaY Zeolite Catalysts

R. CID,* F. J. GIL LLAMBÍAS,† J. L. G. FIERRO,‡ A. LÓPEZ AGUDO,‡ AND J. VILLASEÑOR*

Facultad de Ciencias, Universidad de Concepción, Concepción, Chile, †Departamento de Química, Facultad de Ciencias, Universidad de Santiago de Chile, Santiago, Chile, and ‡Instituto de Catálisis y Petroleoquímica, C.S.I.C., Madrid 6, Spain

Received January 23, 1984; revised May 21, 1984

A series of Mo-impregnated NaY zeolite catalysts, with a Mo loading in the range 1–15 wt%, MoO_3, have been studied by X-ray diffraction, transmission electron microscopy, ir and diffuse reflectance spectroscopy, temperature-programmed reduction, specific surface area, water content, and extraction measurements, in order to characterize them structurally. The crystallinity, specific surface area, and water content of the Mo-NaY were found to decrease almost linearly with increasing Mo loading. These effects were accompanied by an increasing perturbation of the zeolite framework. The ir spectra and, particularly, the diffuse reflectance spectra suggest that Mo is predominantly present as a tetrahedrally coordinated MoO_4^{2-} species, presumably within the zeolite cavities. The Mo extraction and temperature-programmed reduction results revealed the existence of a strong interaction between Mo species and zeolite, which apparently decreases with increasing Mo loading.

INTRODUCTION

Molybdenum compounds deposited on solid supports are being widely used as catalysts in a variety of reaction systems and industrial processes. The most commonly used supports are silica-alumina and, especially, γ-alumina, because molybdenum is highly dispersed on the alumina surface due to the strong chemical interaction between MoO_3 and alumina. In this respect zeolites also seem to be very promising as a support for molybdenum. Moreover, zeolites have exceptional properties, including catalytic activity and greater resistance to poisoning by sulfur- and nitrogen-organic compounds than amorphous silica-alumina-based catalysts. Thus, in recent years an increasing interest in molybdenum-containing zeolite catalysts has developed (*1–10*). In most of the works (*1–6*) molybdenum was loaded on Y or ZSM-5 zeolites by a conventional impregnation technique with an aqueous solution of ammonium heptamolybdate, and their catalytic activities for different reactions were compared with those of other conventional supported molybdenum catalysts, such as Mo/γ-Al_2O_3, Mo/SiO_2, and Mo/silica-alumina.

In most of the reported fundamental studies (*1–4*), no characterization of the Mo-impregnated zeolite catalysts was carried out. Although in a few studies some characterization of the samples was made (*5, 6*), little attention was given to their crystallinity. Thus, for example, the change of Mo coordination from octahedral to tetrahedral in Co- and Mo-containing Y-type zeolite upon reduction by H_2 has been recently shown by diffuse reflectance spectroscopy (*6*). However, the crystallinity of the samples, and Mo location (zeolites cavities or on the external surface) were not clarified. In contrast, for Mo-exchanged Y-type zeolites a detailed characterization study by ir spectroscopy, EPR, XPS, and X-ray diffraction has been recently published by Dai and Lunsford (*8*); they concluded that some loss in crystallinity occurred when Mo ions were introduced into

0021-9517/84 $3.00

Y zeolite using a solid-phase exchange method. In addition, Yashima *et al.* (*10*) also found that the crystal structure of MoY prepared by adsorption of $Mo(CO)_6$ vapor on HY was destroyed to a small extent.

In view of the above and the great practical importance of the zeolite-based Mo hydroprocessing catalysts, the characterization of Mo-impregnated NaY zeolite is of interest. In this paper the effect of Mo loading on the crystallinity of a series of Mo-impregnated NaY zeolites was studied using X-ray diffractions, ir spectroscopy, transmission electron microscopy (TEM), and surface area and water content measurements. In order to examine the Mo dispersion and the possible location of Mo ions in the zeolite, additional measurements of Mo extraction by ammonia solution, diffuse reflectance spectroscopy, and temperature-programmed reduction were also carried out.

EXPERIMENTAL

Sample preparation. Samples of Mo-NaY were prepared by impregnation of NaY zeolite (SK-40 Linde) with aqueous solutions of ammonium heptamolybdate of the appropriate concentration to obtain MoO_3 loadings of 1, 4, 7, 10, and 15 wt%. The volume of solution used was that necessary to completely wet the zeolite sample. pH of the slurry was between 6.2 and 5.1, depending on the concentration of the ammonium heptamolybdate solution. The water was evaporated at 70°C under vacuum in a rotary evaporator. The samples were dried at 110°C overnight, followed by heating at 380°C for 3 h and then calcined at 550°C for 4 h. The sample obtained are designated Mo(x)-NaY, where x indicates the content of MoO_3 per 100 g of NaY. As reference a 15 wt% MoO_3 : NaY physical mixture was prepared by adding both components to 250 ml *n*-pentane and stirring in an ultrasonic bath for 10 min. Solvent was then removed by the freeze-drying method; and the solid was subsequently dried at 110°C for 2 h.

METHODS

Specific surface areas of the samples were obtained by the BET method from the adsorption isotherm at liquid nitrogen temperature, −195°C, and taking a value of 0.162 nm^2 for the cross-sectional area of N_2 molecule at this temperature. Contents of total water in the samples were determined from the weight loss upon calcination at 600°C for 8 h.

X-Ray powder diffraction patterns were obtained on a Philips PW-1010 diffractometer using Cu$K\alpha$ radiation, under constant instrumental conditions. Infrared spectra in the 1400–200 cm^{-1} region were recorded in a Perkin-Elmer 237 B spectrophotometer. Self-supporting wafers of similar thickness (30 mg cm^{-2}) were prepared by pressing an identical amount of powdered zeolite samples diluted with KBr in the proportion 1 : 100. Transmission electron microscopy was carried out in a Philips EM-200 microscope. Specimens were prepared by a carbon replica method. Diffuse reflectance spectra were recorded at room temperature in the 200–500 nm range in a Pye-Unicam SP 1800 spectrophotometer equipped with a SP-890 diffuse reflectance accessory, using as reference NaY zeolite.

Extraction of Mo by solubilization was carried out by treating the samples (0.5 g) with 100 ml of diluted ammonia solution (3% vol) for 48 h. The solubilized Mo was determined in the filtrate by atomic absorption spectrometry. Temperature-programmed reduction by hydrogen was measured by means of a Cahn microbalance. The samples were previously dried in vacuum at 350°C until constant weight, followed by cooling to room temperature, then reduced by hydrogen at a static pressure of 300 Torr while the temperature was linearly increased up to 500°C at a rate of 4°C min^{-1}, and finally the samples were maintained at 500°C for 1 h.

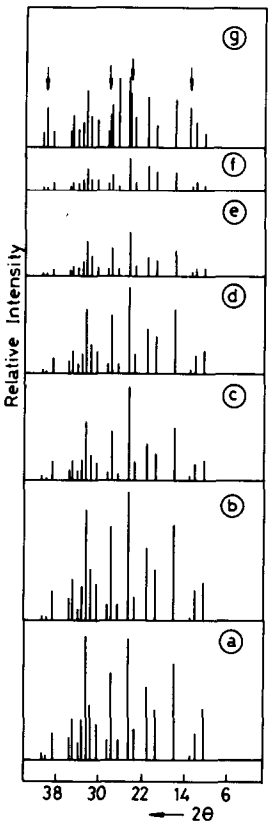

FIG. 1. X-Ray diffraction patterns of a, NaY; b, Mo(1)-NaY; c, Mo(4)-NaY; d, Mo(7)-NaY; e, Mo(10)-NaY; f, Mo(15)-Na; g, 15 wt% MoO_3-NaY physical mixture.

RESULTS AND DISCUSSION

X-Ray Diffraction

Powder diffractograms of Mo(x)-NaY samples and the starting NaY zeolite were recorded over a range of 2θ values from 2 to 60°. Their simplified diffraction patterns for 2θ between 6 and 40°, together with that of the physical mixture of NaY + 15% MoO_3, are compared in Fig. 1. The diffraction peak intensities decrease with increasing Mo loading. This attenuation in the diffraction peaks as compared with the physical mixture cannot be exclusively attributed to absorption and dilution effects caused by high Mo loading. Some loss of crystallinity evidently took place in the Mo(x)-NaY samples. The average changes in crystallinity of the Mo(x)-NaY samples with reference to the intensity of the three most intense peaks (5.71, 3.71, and 2.85 Å) of the starting NaY zeolite were determined and plotted against Mo loading (Fig. 2). Crystallinity decreases almost linearly with increasing Mo loading, the loss of crystallinity being severe for the Mo(15)-NaY sample, as determined by the relatively small peak height. However, since no corrections were made for the possible absorption and dilution effects, the values of Fig. 2 are probably too low. It is to be noticed that using the same criterion for crystallinity determination, the value found for the physical mixture was approximately 65% relative to the 100% of the NaY sample, although no loss of crystallinity took place in the physical mixture.

Detailed analysis of the X-ray diffraction pattern of the samples did not show evidence of a MoO_3 phase. If a small amount of MoO_3 were present, its detection would be very difficult because the more intense peaks of MoO_3 (d-spacings of 6.93, 3.81, 3.46, 3.26, 2.31 Å) are very close or coincident with those of NaY (7.37, 6.91, 3.71, 3.45, 3.31, and 2.28 Å). Only when the amount of MoO_3 is relatively high, as, e.g., in the case of the physical mixture shown in Fig. 1, some differences in the pattern (mainly in relative peak intensities, marked by arrows in Fig. 1) can be distinguished.

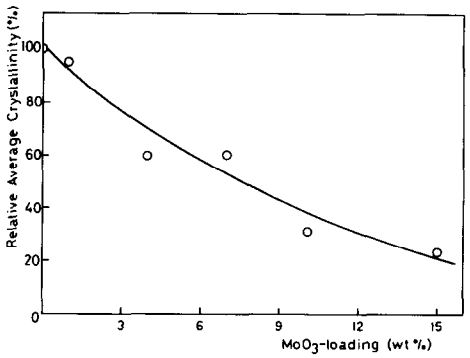

FIG. 2. Effect of Mo loading on relative average crystallinity (as measured by X-ray diffraction) of Mo(x)-NaY samples.

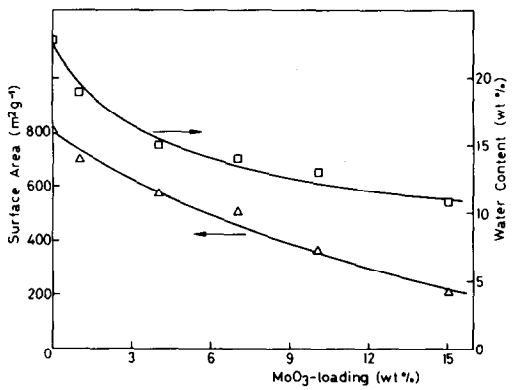

FIG. 3. Effect of Mo loading on surface area (△) and water content (□) of Mo(x)-NaY samples.

However, as X-ray diffraction only reveals crystallites above a certain minimum size (~40 Å), the presence of MoO_3 species in the Mo(x)-NaY samples cannot be unambiguously excluded based only on this technique, particularly in the sample with the highest Mo loading.

Surface Area and Content of Zeolite Water

The surface area and water content are used here as another measure of the crystallinity of the samples. Figure 3 summarizes the results. Both the surface area and the total content of water in the samples decreased almost linearly with increasing Mo loading. These changes cannot be explained by dilution since the physical mixture of NaY + 15% MoO_3 gave a surface area of 675 m^2 g^{-1} and a water content of 23.4%, which correspond quite closely to the expected values considering the dilution of the NaY sample. The possibility that both decreases in surface area and water content could be only due to a partial blockage of zeolite cavities by deposit of polymolybdate in the external surface is also quite unlikely. If such effect occurred no change in the X-ray diffraction pattern should have been found because it cannot affect the zeolite structure. Thus, the decreases in surface area and water content are indicative of a progressive decomposition of the zeolite structure, as the X-ray diffraction patterns also suggest.

Figure 4 shows that there is a rough correlation between relative change of surface area or water content and X-ray diffraction crystallinity. Some of the experimental points are slightly over the theoretically expected line when surface area, water content, and crystallinity decreased to exactly the same extent. The dispersion, which is more manifest in the samples with high Mo loading, is probably due to the lowering of the X-ray diffraction crystallinity values pointed out above as a result of absorption and dilution effects.

TEM

Conventional TEM micrographs of the samples are shown in Fig. 5. The samples with low Mo loadings, i.e., Mo(1)-NaY and Mo(4)-NaY showed (Figs. 5a and b) only the typical morphology of gains of crystallized NaY. As the Mo loading increased small grains of material apparently poorly crystallized were observed. In the case of the Mo(15)-NaY sample, some particles showing a morphology slightly different from that of the NaY zeolite and resembling that of MoO_3 crystals were also observed. However, the contrast with the other aggregates was not enough to ensure the presence of a MoO_3 phase. Interestingly, this uncertainty also remained in the micro-

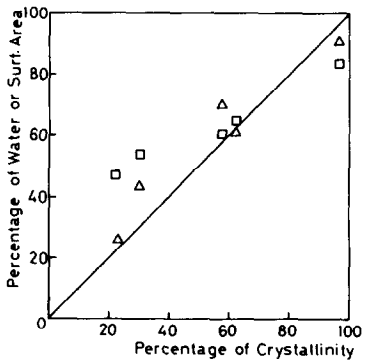

FIG. 4. Relationship between relative average crystallinity and surface area (△) or water content (□) of the Mo(x)-NaY samples.

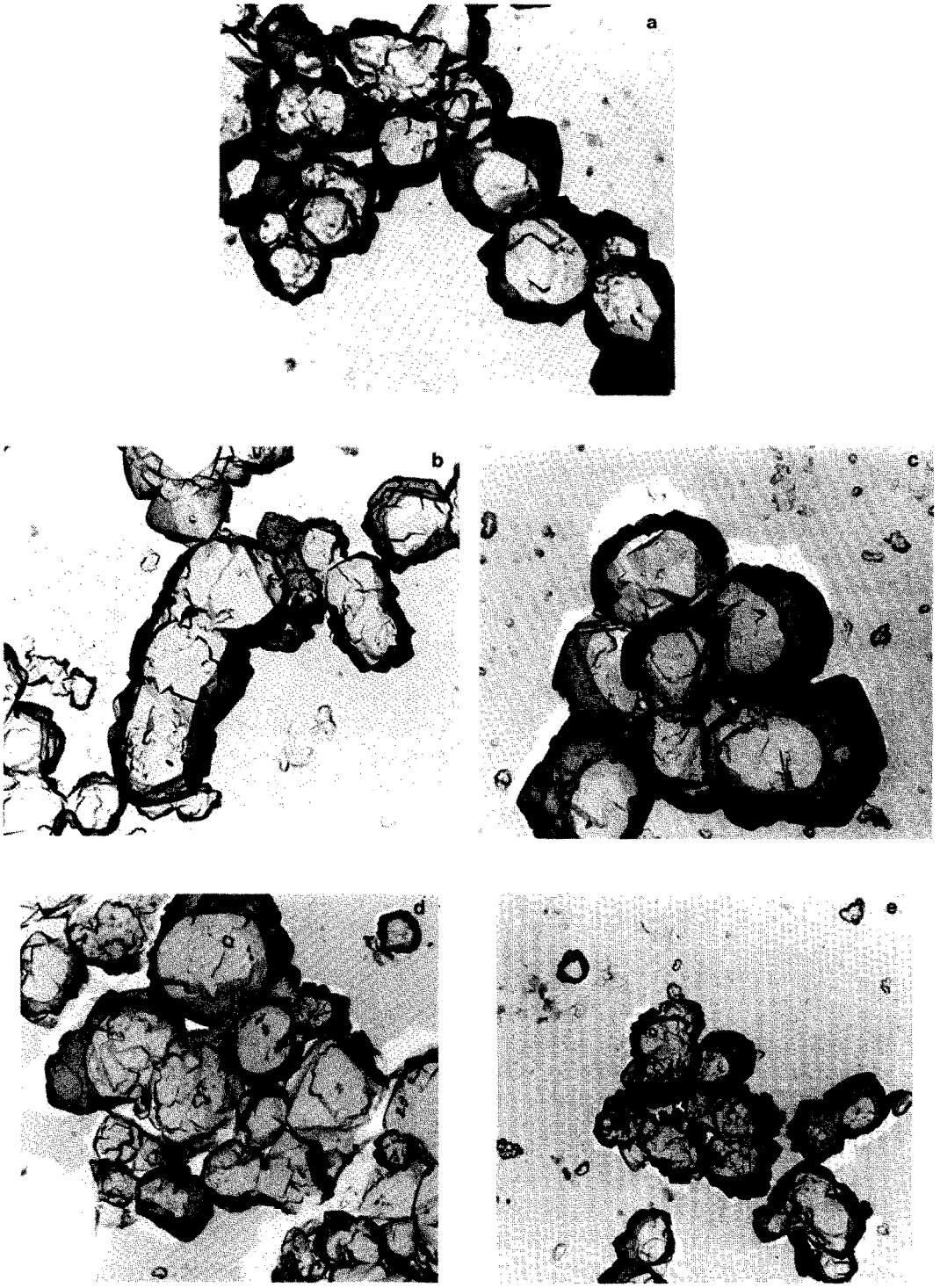

FIG. 5. TEM micrographs of the samples: (a) Mo(1)-NaY; (b) Mo(4)-NaY; (c) Mo(7)-NaY; (d) Mo(10)-NaY; (e) Mo(15)-NaY.

graphs of the physical mixture. In view of this, we tried to obtain the electron diffraction patterns (under the electron beam of the microscope) of the Mo(15)-NaY sample and of the physical mixture. It should be noticed that the electron diffraction patterns were only feasible when the beam was aimed at the boundary of the aggregates. After re-examining about 30 diffraction patterns corresponding to aggregates present in the same microscope field no clear evidence was obtained on the presence of two separate phases, i.e., Mo-NaY and MoO_3 in the Mo(15)-NaY sample. Furthermore, the physical mixture exhibited two types of electron diffraction pattern of MoO_3: weak and intense diffraction, depending on the aggregates. The weak diffraction is probably due to a small amount of MoO_3 bound to NaY, which results from the preparation of the physical mixture in the presence of the remaining molecular water of the NaY zeolite. The intense diffraction pattern corresponds to the MoO_3 phase.

Diffuse Reflectance Spectra

Figure 6 shows the diffuse reflectance spectra between 190 and 360 nm for the Mo-loaded NaY zeolites. All the samples except the Mo(1)-NaY exhibited clearly two bands about 230 and 266 nm, similar to those found for molybdena supported on γ-Al_2O_3, which are attributable to Mo^{6+} ions in tetrahedral (monomeric) and octahedral (polymeric) coordination with oxide ions (*11–14*). The Mo(1)-NaY developed, however, only a broad band centered at about 220 nm accompanied by a weak absorption between 250 and 310 nm. The two bands at about 230 and 266 nm increase in intensity with increasing Mo loading, the second one more so than the first. In addition, the band about at 266 nm appears clearly asymmetric toward longer wavelengths, suggesting some contribution of a band positioned above 270 nm. We presume that such a band could be the third one characteristic of polymeric Mo^{6+} in octahedral coordination which appears between 300 and 250 nm (*11–14*). According to the literature (*11–14*), the precedent spectral features indicate that Mo is present in the samples as Mo^{6+} in both octahedral and tetrahedral coordination with oxide ions. Although the octahedral species increase with increasing Mo loading, on the basis that no clear band or shoulder appeared above 300 nm, even in the Mo(15)-NaY sample, the dominant Mo species are probably tetrahedral MoO_4^{2-} anions bound to the zeolite framework.

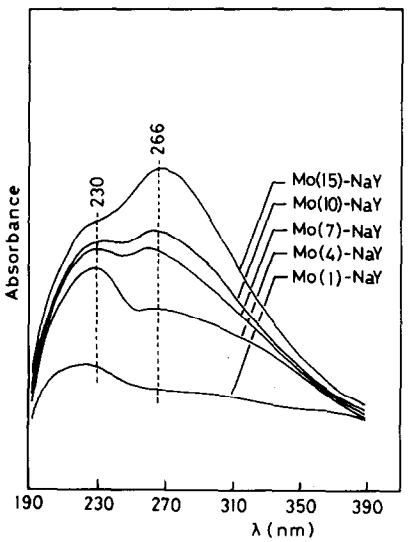

FIG. 6. Ultraviolet diffuse reflectance spectra of Mo(x)-NaY samples.

A broad band near 330 nm which appears to be characteristic of MoO_3 (*12–14*) was not observed in the spectra in agreement with the absence of MoO_3 peaks in the X-ray diffractograms.

Mid-Infrared Spectra

The framework ir spectra of all the Mo(x)-NaY samples and the parent NaY zeolite, as well as that of the physical mixture NaY–15 wt% MoO_3, are shown in Fig. 7. All Mo-loaded samples exhibited bands of varying intensity and width, depending on the Mo loading, at about 1140, 1010, 785, 705, 580, 465, and 380 cm^{-1}, which are typical for NaY (*15, 16*). Samples with Mo loadings over 4% MoO_3 also exhibited an additional broad and weak band centered

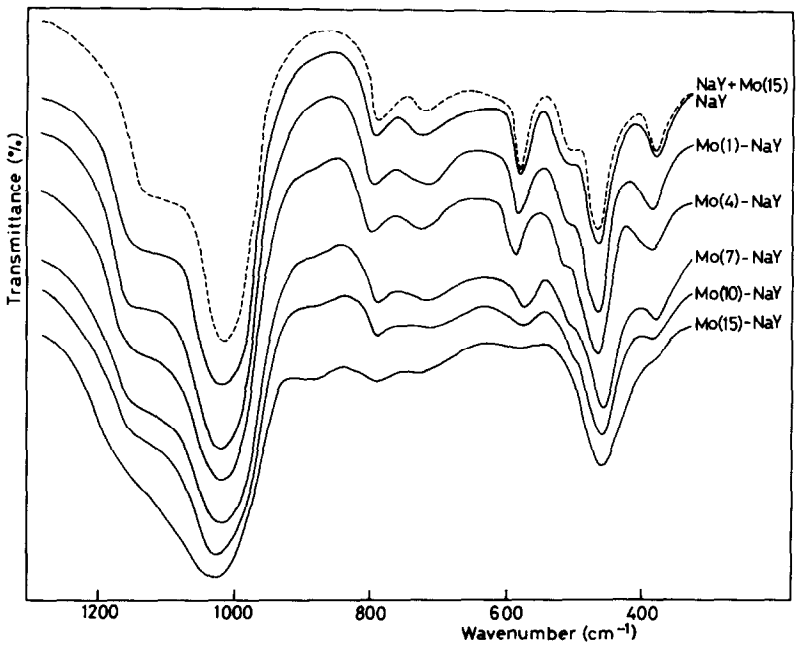

FIG. 7. Framework infrared spectra of NaY zeolite, Mo(x)-NaY samples, and 15 wt% MoO_3-NaY physical mixture.

around 890 cm^{-1}, whose intensity increased with increasing Mo loading. The features of the physical mixture spectrum were practically the same as those of the NaY, no significant changes being detected.

The bands at about 1010, 705, and 465 cm^{-1} are caused by internal vibrations of the (Si, Al)O_4 tetrahedra of NaY, which tend to be insensitive to structure variations, whereas the bands at about 1140, 785, 580, and 380 cm^{-1} are due to vibrations related to external linkages between tetrahedra, and are sensitive to the framework structure (*15, 16*). As shown in Fig. 7, the strong bands at about 1010 and 465 cm^{-1} appeared in all the Mo(x)-NaY samples, with minor changes an intensity, width, and position as Mo loading increased. The more relevant of these minor changes occurred in the main asymmetric stretching vibration at about 101 cm^{-1}, which showed a decrease in intensity, a broadening, and a slight shift towards higher frequencies with increasing Mo loading. In contrast, the structure-sensitive bands at about 1140, 785, 580, and 380 cm^{-1} decreased significantly in intensity when Mo loading increased. The changes are more evident when we compare, for example, the spectra of the Mo(1)-NaY and Mo(15)-NaY samples. In the latter the structure-sensitive bands were almost or completely removed. It is remarkable that the well-resolved band appearing at 380 cm^{-1} in the Mo(1)-NaY, which is related to the opening pore of the NaY, is only apparent as a shoulder in the spectrum of the Mo(15)-NaY. In general, all the changes observed in the position and intensity of the bands, especially in the structure-sensitive bands, are indicative of a perturbation of the zeolite framework, which increases substantially with increasing Mo loading. This conclusion is in excellent agreement with the surface area and the X-ray diffraction results. Similar perturbation in the zeolite structure were also shown by ir for a series of thermally degraded NaY zeolites with different X-ray crystallinities (*16*) and for MoHY zeolites prepared by cation exchange (*8*).

Regarding the new broad band appearing at about 890 cm^{-1}, since it was absent in the parent NaY zeolite, it is then reasonable to associate it to some molybdenum oxygen bond vibration. The assignment of this band on the basis of similarity with reference compounds is, however, not unambiguous, and various interpretations for bands very close to that observed in the present work have been proposed (*7, 8*). For example, Dai and Lunsford (*8*) attributed a band at 900 cm^{-1}, which appeared in MoHY zeolites prepared from $MoCl_5$, to an Mo=O bond vibration of an oxo-molybdenum complex ions located at S_{II} sites. However, Gallezot *et al.* (*7*) attributed the band observed at 895 cm^{-1} in $Mo(Co)_6$ adsorbed on HY zeolites to Mo—O vibrations similar to those observed for Mo oxides. In addition, it should also be pointed out that MoO_3 gives two characteristic strong ir bands at 865 and 990 cm^{-1} (*12*). If such a phase was present in Mo(*x*)-NaY samples the 990 cm^{-1} band would be overwhelmed by the stronger one near 1000 cm^{-1} of the NaY, and the 865 cm^{-1} band would be slightly shifted to a higher wavelength by the interaction with the zeolite surface. In fact, the two bands of MoO_3 were not found in the spectrum of the physical mixture NaY + 15% MoO_3 (Fig. 7). Since MoO_3 species were not detected in the Mo(*x*)-NaY samples by either X-ray diffraction or diffuse reflectance spectroscopy, the assignment of the 890 cm^{-1} band to MoO_3 is, therefore, very unlikely. In contrast, the diffuse reflectance spectra of the sample suggest the existence of Mo^{6+} predominantly in tetrahedral coordination. We thus consider more reasonable to assign the band at about 890 cm^{-1} to a Mo=O bond vibration of monomeric MoO_4^{2-} species attached to the zeolite framework. The presence of a similar tetrahedrally coordinated CrO_4^{2-} species within the supercages of zeolites without a substantial collapse of the lattice is known to exist in oxidized chromium-exchanged zeolites (*17*). Thus, we conclude from the infrared results that a progressive instabilization of the structure zeolite is produced by increasing Mo loading. Molybdate species may be present into the supercages of the zeolite, and upon dehydration and dehydroxylation they may be bounded to oxygen from the zeolite lattice, causing a substantial partial breakdown of the zeolite framework when the Mo loading is relatively high.

TABLE 1

Percentages of Extracted Mo by Ammonia Solution

Sample	Extracted Mo (%)
Mo(1)-NaY	30
Mo(4)-NaY	28
Mo(7)-NaY	37
Mo(11)-NaY	34
Mo(15)-NaY	40

Extraction of Molybdenum by Ammonia

The extracted Mo expressed as percentage of Mo loading of the samples is given in Table 1. There a slight tendency for the percentage of extracted Mo to increase as the Mo loading in the samples increases, i.e., the proportion of Mo not strongly attached to the zeolite surface increases with Mo loading. This increase in extracted Mo is consistent with the increase of Mo octahedrally coordinated shown by diffuse reflectance spectra with increased Mo loading, and with the lower temperature for initial reduction of the high-Mo-loading sample as described below. The relatively large fraction (over 60%) of Mo strongly retained in the zeolite after extraction, and the fact that bulk MoO_3 is readily dissolved by ammonia solution (*12*), suggests that such Mo fraction may be within the zeolite cavities, interacting strongly with their lattice oxygen ions.

Comparison of extracted Mo in Mo(*x*)-NaY samples and in alumina-supported molybdena catalysts (*18, 19*) shows that the percentage of extracted Mo was approximately higher by a factor 2 in the alumina-

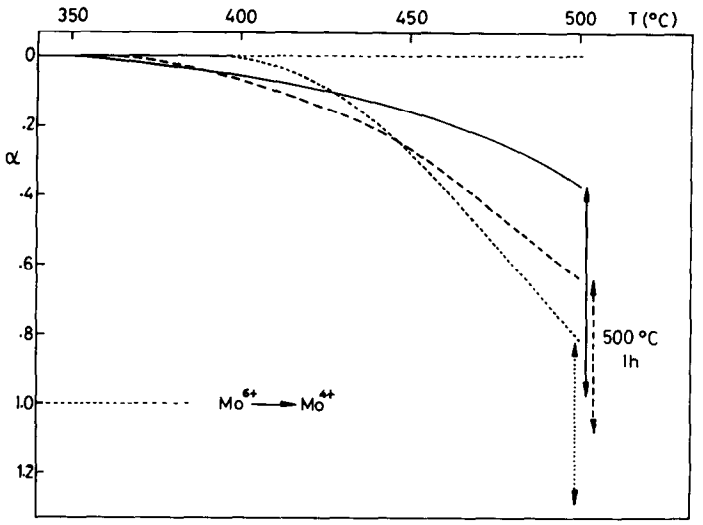

FIG. 8. Temperature programmed reduction (as reduction degree, α) for the Mo(4)-NaY, Mo(7)-NaY, and Mo(15)-NaY samples.

supported catalysts than in the Mo(x)-NaY samples. This difference in extracted Mo is significant and could be explained either on the basis of a stronger interaction of the Mo with the zeolite surface as compared with the alumina or as being due to a higher dispersion of Mo on zeolite than on alumina due the larger specific surface area of the first. Since the specific surface area of the Mo(15)-NaY sample (210 m^2g^{-1}) was, however, not significantly larger than that of an alumina-supported sample (180 m^2g^{-1}) with a similar Mo loading in Ref. (*19*). Then, both samples may have a similar surface coverage. However, the percentages of extracted Mo were 40 and 79 for the Mo(15)-NaY and the Mo(14.3)/Al_2O_3 of Ref. (*19*), respectively. Thus, the difference in extracted Mo between the alumina and zeolite-supported Mo samples is more likely due to differences in the strength of interaction between the Mo species and the two supports rather to differences of Mo dispersion.

Temperature-Programmed Reduction

The results of temperature-programmed reduction by H_2 of the Mo(4)-NaY, Mo(7)-NaY, and Mo(15)-NaY samples, expressed as of reduction α, are summarized in Fig. 8. The extent of reduction α was defined as the ratio of the experimental to theoretically calculated weight loss of the samples upon reduction, assuming as theoretical weight loss that corresponding to the quantitative reduction of MoO_3 to MoO_2.

As shown in Fig. 8, the temperature at which the reduction starts for the sample with higher Mo loading is 350°C while for the lowest Mo loading it is 400°C. The initial temperature of reduction clearly decreases with increasing Mo loading. A similar effect with increasing surface coverage was observed in alumina-supported molybdena catalysts (*20–22*). This decrease in reduction temperature is interpreted as due to differences in the strengths of interaction between the zeolite and the molybdate ions, the interaction being stronger when Mo loading decreases and Mo is predominantly tetrahedrally coordinated, as the diffuse reflectance spectra of Fig. 6 suggest. These observations are consistent with the well known phenomenon that Mo supported on alumina in tetrahedral coordination symmetry is less reducible than in octahedral coordination symmetry (*23–25*).

Inspection of Fig. 8 shows that the reduction proceeds differently on the three samples studied, several crossovers appearing in the reduction curves. The extent of reduction increases with the temperature and very rapidly when the Mo loading of the sample decreases. Such a reduction behavior leads then to a higher extent of reduction at temperatures over 470°C for the less Mo-loaded sample, which is, however, less reducible according to its starting temperature of reduction. This apparent contradiction can be accounted for by considering the differences of surface coverage, Mo dispersion, and particle size of the supported species. It is expected that after reduction has started a high dispersion of the supported molybdate species, as occurs in the Mo(4)-NaY sample, may favor their reduction. In the case of samples with higher Mo loadings, we have seen that the presence of a small fraction of octahedral Mo in multilayers and/or as bulk MoO_3 is probable. Since an induction time usually appears in the reduction of bulk MoO_3 (*26, 27*), if small microcrystals of MoO_3 were present in the Mo(15)-NaY sample their reduction would proceed more slowly.

Under the conditions of reduction used some of the hydrogen is irreversibly retained by the support, as has been shown in molybdena catalysts supported on alumina (*20, 25*). Besides, if the water formed in the reduction is not completely eliminated, it could reoxidize reduced Mo (*28*). In either case, the observed variation of α after reduction begins could not be representative of the real reducibility of the samples since α was measured by their weight loss upon reduction, whereby several possible effects could be included. As such effects may be negligible at the beginning of the reduction, the temperature of incipient reduction may better reflect the reducibility of the samples. Therefore, a greater resistance to initial reduction of Mo(4)-NaY may be due to the presence of Mo species predominantly in tetrahedral coordination.

CONCLUSIONS

The results presented in this work show that the preparation of Mo-containing NaY zeolite samples by impregnating NaY with aqueous solutions of ammonium heptamolybdate results in a loss in crystallinity and surface area. Although the loss in both crystallinity and surface area is apparently substantial for samples with Mo loadings beyond 7 wt% MoO_3, no clear evidence for a complete breakdown of the zeolite structure and for the presence of a MoO_3 phase was found, even for the sample containing 15% MoO_3. At relatively low Mo loadings, Mo species appear to be well dispersed on the zeolite, mostly within the zeolite cavities as strongly attached tetrahedrally coordinated MoO_4^{2-}.

ACKNOWLEDGMENT

The authors acknowledge the financial support of the Dirección de Investigación de la Universidad de Concepción, Chile (Project No. 201302), and the CAICYT of Spain.

REFERENCES

1. Golding, R., Molnar, E., Abrams, O., Katan, L., and Arenas, B., *in* "Proceedings of the Vth Iberoamerican Symposium on Catalysis" (M. Farinha Portela and Carlos M. Pulido, Eds.), Vol. II, p. 203. Lisbon, 1979.
2. Vysotskii, A. V., Chuikova, N. A., and Lipovich, V. G., *Kinet. Katal.* **18,** 1345 (1977).
3. Wilhelm, F. C., Tsigdinos, G. A., and Ference, R. A., *in* "Proceedings of the Climax Third International Conference on the Chemistry and Uses of Molybdenum" (H. F. Barry and P. C. H. Mitchel, Eds.), p. 219. Climax Molybdenum Company, Ann Arbor, Michigan, 1979.
4. Swanson, W. W., Strensand, B. J., and Tsigdinos, G. A., *in* "Proceedings of the Climax Fourth International Conference on the Chemistry and Uses of Molybdenum" (H. F. Barry and P. C. H. Mitchel, Eds.), p. 323. Climax Molybdenum Company, Ann Arbor, Michigan, 1982.
5. Balakrishnan, I., Hedge, S. G., Rao, B. S., Kulkarni, S. B., and Ratnasamy, P., *in* "Proceedings of the Climax Fourth International Conference on the Chemistry and Uses of Molybdenum" (H. F. Barry and P. C. H. Mitchell, Eds.), p. 331. Climax Molybdenum Company, Ann Arbor, Michigan, 1982.

6. Kovacheva, P., Davidova, N., and Shopov, D., *Zeolites* **3,** 92 (1983).
7. Gallezot, P., Coudurier, G., Primet, M., and Imelik, B., *in* "Molecular Sieves II2 (J. R. Katzer, Ed.). *Amer. Chem. Soc. Symp. Ser.* **40,** 144 (1977).
8. Dai, P. S. E., and Lunsford, J. H., *J. Catal.* **64,** 173 (1980).
9. Dai, P. S. E., and Lunsford, J. H., *J. Catal.* **64,** 184 (1980).
10. Yashima, T., Komatsu, T., and Namba, S., *in* "Proceedings of the Climax Fourth International Conference on the Chemistry and Uses of Molybdenum" (H. F. Barry and P. C. H. Mitchell, Eds.), p. 274. Climax Molybdenum Company, Ann Arbor, Michigan, 1982.
11. Ashley, J. H., and Mitchell, P. C. H., *J. Chem. Soc. A.,* 2821 (1968), 2730 (1969).
12. Giordano, N., Bart, J. C. J., Vaghi, A., Castellan, A., and Martinotti, G., *J. Catal.* **36,** 81 (1975).
13. Jeziorowski, H., and Knözinger, H., *J. Phys. Chem.* **83,** 1166 (1979).
14. Wang, L., and Hall, W. K., *J. Catal.* **77,** 232 (1982).
15. Scherzer, J., and Bass, J. L., *J. Catal.* **28,** 101 (1973).
16. Flanigen, E. M., and Khatami, H., *Adv. Chem. Ser.* **101,** 201 (1971).
17. Coughlan, B., McCann, W. A., and Caroll, W. M., *J. Colloid Interface Sci.* **74,** 136 (1980).
18. Gil, F. J., Mendioroz, S., and López Agudo, A., *Bull. Soc. Chim. Belg.* **90,** 1331 (1982).
19. Fierro, J. L. G., Gil Llambías, F. J., López Agudo, A., and Rives Arnau, V., *in* "Proceedings 8th Iberoamerican Symposium on Catalysis, La Rábida (Huelva), 1982," Vol. II, p. 615.
20. Massoth, F. E., *J. Catal.* **30,** 204 (1973).
21. Yao, H. C., *J. Catal.* **70,** 440 (1981).
22. Thomas, R., van Oers, E. M., de Beer, V. H. J., Medema, J., and Moulijn, J. A., *J. Catal.* **76,** 241 (1982).
23. Chung, K. S., and Massoth, F. E., *J. Catal.* **64,** 320 (1982).
24. Medema, J., Van Stam, C., de Beer, V. H. J., Konings, A. A. A., and Koningsberger, D. C., *J. Catal.* **53,** 386 (1978).
25. Hall, W. K., *in* "Proceedings of the Climax Fourth International Conference on the Chemistry and Uses of Molybdenum" (H. F. Barry and P. C. H. Mitchell, Eds.), p. 224. Climax Molybdenum Company, Ann Arbor, Michigan, 1982.
26. Gajardo, P., Grange, P., and Delmon, B., *J. C. S. Faraday I* **76,** 929 (1980).
27. Fierro, J. L. G., Soria, J., and López Agudo, A., *Appl. Catal.* **3,** 117 (1982).
28. Peri, J. B., *J. Phys. Chem.* **86,** 1615 (1982).